

# Nuclear structure far from stability

D. Vretenar <sup>a</sup>

<sup>a</sup>Physics Department, Faculty of Science, University of Zagreb, Croatia

Modern nuclear structure theory is rapidly evolving towards regions of exotic short-lived nuclei far from stability, nuclear astrophysics applications, and bridging the gap between low-energy QCD and the phenomenology of finite nuclei. The principal objective is to build a consistent microscopic theoretical framework that will provide a unified description of bulk properties, nuclear excitations and reactions. Stringent constraints on the microscopic approach to nuclear dynamics, effective nuclear interactions, and nuclear energy density functionals, are obtained from studies of the structure and stability of exotic nuclei with extreme isospin values, as well as extended asymmetric nucleonic matter. Recent theoretical advances in the description of structure phenomena in exotic nuclei far from stability are reviewed.

## 1. Introduction

Experimental and theoretical studies of nuclei far from stability are at the forefront of modern nuclear science. Prompted by a wealth of new experimental data on exotic nuclei with extreme isospin values, by the rich astrophysical phenomenology, as well as theoretical developments in related fields, important qualitative and quantitative advances in theoretical nuclear structure have recently been reported. Modern nuclear structure theory is rapidly evolving from macroscopic and microscopic models of stable nuclei towards regions of short-lived nuclei close to the particle drip lines. Accurate global microscopic calculations have become standard in astrophysical applications, and a series of studies based on concepts of effective field theory has been initiated in order to bridge the gap between low-energy non-perturbative QCD and nuclear many-body dynamics.

In light systems quantum Monte Carlo calculations have been extended to  $A \leq 12$  nuclei and to neutron droplets, and the *ab initio* no-core shell model approach currently provides a quantitative description of  $p$ -shell nuclei. Large-scale shell model calculations have been performed for medium-heavy and heavy nuclei, and applied to problems relevant to nuclear astrophysics. In the microscopic description of weakly bound neutron-rich nuclei, improved shell model techniques allow for a consistent treatment of bound states, resonances and the non-resonant continuum background.

Global shell-model approaches and microscopic self-consistent mean-field models have been very successful in the description of the evolution of shell structure, the disappearance of spherical magic numbers, deformations and shape coexistence in exotic nuclei. The evolution of quadrupole collectivity and the coexistence of shapes have been analyzed with self-consistent models that include correlations beyond the mean-field approxima-

tion. Microscopic mass formulas based on the self-consistent HFB framework have been developed. The covariant mean-field framework has been extended with explicit density-dependent effective interactions, which provide an improved description of asymmetric nuclear matter, exotic nuclei, hypernuclei, and neutron star matter.

New theoretical tools have been developed to describe the multipole response of neutron-rich nuclei. Several implementations of the (continuum) non-relativistic and relativistic quasiparticle random-phase approximation, as well as the shell model and the quasiparticle phonon model, have been employed in studies of the evolution of the low-energy dipole and quadrupole response in nuclei with a large neutron excess.

## 2. *Ab initio* and global shell-model description of light nuclei

Light and medium-light nuclei play a particularly important role in modern nuclear structure. Experimentally, these nuclei are accessible from the proton to the neutron drip line and, therefore, provide information on systems with extreme  $N/Z$  ratios. Their structure can be analyzed with a variety of theoretical approaches, including exact *ab initio* calculations with NN and NNN bare interactions. Neutron-rich light nuclei exhibit very interesting structure phenomena, such as the weak binding of the outermost neutrons, pronounced effects of the coupling between bound states and the particle continuum, regions of nuclei with very diffuse neutron densities, formation of halo structures.

In the past few years a number of microscopic studies have shown that accurate predictions about the stability, structure and reactions of light nuclei can be made starting from the interactions among individual nucleons. Energies of all the bound and narrow states of up to ten nucleons can be reproduced almost exactly (within 2%) by employing bare nuclear forces that fit NN scattering data, with the addition of realistic NNN forces. The most accurate *ab initio* calculations of ground states and low-lying excitations of light nuclei, starting from realistic models of the nuclear force, use the Quantum Monte Carlo (QMC) method [1]. Most of the QMC calculations have been performed using the Argonne  $v_{18}$  (AV18) NN potential [2], alone or with the inclusion of NNN potentials. The AV18 is representative of the modern NN potentials that give accurate fits to scattering data. However, with the exception of  ${}^2\text{H}$ , NN potentials alone cannot describe the structure of light nuclei. It has been known for a long time that Hamiltonians containing only realistic NN potentials underbind the light nuclei, overestimate the equilibrium density of nuclear matter, and cannot reproduce the empirical energy spacings between spin-orbit partner levels. Already three- and four-nucleon systems provide ample evidence for the presence of NNN interactions in nuclei. In addition to increasing the total binding energy, the inclusion of NNN interactions improves the level ordering and level spacing among low-energy states in comparison with experimental spectra and, especially important, enhances the spin-orbit effects. In contrast to the NN interaction, however, a detailed form and parameterization of the NNN forces are not well established. QMC nuclear structure calculations have recently been used to construct a set of improved pion-exchange NNN potentials, designated the Illinois models [3], by fitting the energies of all the 17 bound or narrow states of  $3 \leq A \leq 8$  nuclei. Used in conjunction with the AV18 NN potential, the new Illinois NNN models have been very successfully employed in QMC calculations of ground and low-lying excited states of  $A = 9, 10$  nuclei [4], and of seven- and eight-body

neutron drops in external potential wells [3]. QMC calculations of the ground state of fourteen neutrons in a periodic box, approximating uniform neutron matter, have recently been reported at densities up to one and half times the nuclear matter density [5]. In general, however, the computational effort increases exponentially with the number of nucleons, and with the present computing resources  $^{12}\text{C}$  may be the largest symmetric nucleus that can be calculated in the QMC framework. A new approach, the auxiliary field diffusion Monte Carlo method, has been applied to large neutron systems at zero temperature ( $\approx 60$  neutrons) [6], and should be capable of describing nuclei with  $A > 12$ .

An alternative, complementary approach is the large-basis no-core shell model (NCSM). In this *ab initio* method the effective Hamiltonian is derived microscopically from realistic NN interactions as a function of the finite harmonic oscillator basis space. NCSM calculations have been performed for both *s*-shell and *p*-shell nuclei in large, multi- $\hbar\Omega$  model spaces. The Argonne and CD-Bonn NN potentials have been used in the NCSM calculations of binding energies, excitation spectra, electromagnetic properties and Gamow-Teller transitions of  $A = 10$  nuclei [7]. However, as in the case of QMC calculations, the comparison with experimental data indicates the need for NNN forces. The NCSM has very recently been extended to include effective [8] and realistic [9] NNN interactions in calculations of *p*-shell nuclei. The first applications, using the Argonne V8' NN potential and the Tucson-Melbourne TM'(99) NNN interaction, include *p*-shell nuclei up to  $^{13}\text{C}$ . The inclusion of the NNN interaction increases the calculated binding energies and, in general, the low-lying spectra are in better agreement with experiment. In particular, with the realistic NNN force, the correct ground-state spins are obtained for  $^{10,11,12}\text{B}$  and  $^{12}\text{N}$ , contrary to calculations with NN potentials only. An exciting new development is the recent NCSM calculation of  $^6\text{Li}$  and  $^{10}\text{B}$  [10], using the new, effective field theory (EFT) based, momentum space nonlocal NN potential at the fourth order of the chiral perturbation theory ( $N^3\text{LO}$ ) [11]. The results are consistent with those obtained with standard NN potentials, and identify the need for NNN terms that appear already at the third order of the chiral perturbation theory.

For medium-light nuclei with  $A > 12$  the method of choice, when applicable, is the global shell model approach. The building blocks of the nuclear shell model: the universal effective interactions, a comprehensive treatment of the valence space, and the solution of the secular problem in a finite space, have reached a high level of sophistication and accuracy [12]. It is now possible to diagonalize matrices in determinantal spaces of dimension around  $10^9$  using the Lanczos method. New effective interactions have been constructed that are connected with both the NN and NNN bare forces. The two-body effective interactions are related to realistic NN potentials that fit scattering data, whereas three-body contributions correct the bad saturation and shell-formation properties of realistic two-body forces. It has been shown that with the inclusion of a simple three-body monopole Hamiltonian, large-scale shell-model calculations achieve a very accurate description of low-energy spectra in the *p*, *sd* and *pf* shells [13–15].

The microscopic description of weakly bound and unbound nuclei necessitates a consistent treatment of both the many-body correlations and the continuum of positive energy states and decay channels. The nuclear shell model has recently been extended to allow a treatment of an arbitrary number of valence nucleons occupying the bound states and the particle continuum. The Gamow Shell Model (GSM) [16] has been formulated us-

ing a complex Berggren ensemble representing bound single-particle states, single-particle resonances, and non-resonant continuum states. The model has been successfully tested in calculations involving several valence neutrons outside the doubly-magic core:  ${}^{6-10}\text{He}$  and  ${}^{18-22}\text{O}$  [17], and in the description of  ${}^{5-11}\text{Li}$  including the model space of proton and neutron states [18]. The first results for binding energies, excitation spectra, and electromagnetic properties look very promising. It has been demonstrated that the contribution of the non-resonant continuum is crucial, especially for unbound and near-threshold states. In some cases (e.g.,  ${}^{8,9}\text{He}$ ) non-resonant continuum components dominate the structure of the ground-state wave function. In all cases considered, the GSM calculations yield neutron resonances above the calculated neutron threshold – a feature that is not imposed *a priori* on the model. In contrast to the standard shell model, the effective interactions of GSM cannot be represented as a single matrix calculated for all nuclei in a given mass region. The matrix elements that involve continuum states are strongly system-dependent and they take into account the spatial extension of the single-nucleon wave functions. For future applications it will be important to develop realistic effective interactions to be used in the GSM. It should also be emphasized that the dimension of the non-hermitian Hamiltonian matrix of the GSM grows extremely fast with increasing size of the Hilbert space, and therefore for a successful application of the GSM to heavier nuclei the model basis must be optimized. One promising approach is the implementation of a method based on the density matrix renormalization group [18,19].

### 3. Evolution of shell structure

The phenomenon of shell evolution in exotic nuclei has been the subject of extensive experimental and theoretical studies. Far from the  $\beta$ -stability line the energy spacings between single-particle levels change considerably with the number of neutrons and/or protons. This can result in reduced spherical shell gaps, modifications of shell structure, and in some cases spherical magic numbers may disappear. For example, in neutron-rich nuclei  $N = 6, 16, 34\dots$  can become magic numbers, while  $N = 8, 20, 28\dots$  disappear. The reduction of a spherical shell closure is associated with the occurrence of deformed ground states and, in a number of cases, with the phenomenon of shape coexistence. For particular isotopic chains the onset of deformation could extend the neutron drip line far beyond the limit expected for spherical shapes.

Both the shell model approach and the self-consistent mean-field models have been employed in the description of shell evolution far from stability. The basic advantage of the shell model is the ability to describe simultaneously all spectroscopic properties of low-lying states for a large domain of nuclei. Advances in parallel computer technology, algorithms and computer codes have extended the range of nuclei amenable to a shell model description. Present capabilities include all nuclei in the  $pf$ -shell and the  $f_{5/2}$ ,  $p_{3/2}$ ,  $p_{1/2}$ ,  $g_{9/2}$  valence space, as well as heavy semi-magic nuclei, for instance the  $N = 126$  isotones. The region of deformed nuclei around  $N = Z = 40$  requires a model space that is prohibitively large for diagonalization shell-model approaches, but is feasible in modern stochastic, e.g. Monte Carlo, versions of the shell model.

The origin of the shell evolution and new magic numbers in light exotic nuclei has been attributed to the spin-isospin dependent central part of the effective NN interaction

in nuclei [20]. Although the importance of the  $p - n j_> - j_<$  monopole interaction for the evolution of magicity is still the subject of some debate [21], and it seems that very recent experimental data do not show evidence for some predicted magic numbers in heavier systems (e.g.  $N = 34$  [22]), nevertheless it has been shown that a shell-model Hamiltonian with enhanced spin-flip proton-neutron interaction provides an improved description of Gamow-Teller transitions and magnetic moments in  $p$ -shell nuclei [23]. The spectroscopy of proton-deficient nuclei in the  $sd$  and  $pf$ -shells provides ample evidence that the traditional magic numbers do not extend far from stability. Extensive shell-model and mean-field studies have predicted the erosion of the spherical  $N = 20$  and  $N = 28$  shell closures in neutron-rich nuclei. The results of large-scale shell-model calculations are in very good agreement with the recently determined level schemes of  $^{40,42,44}\text{S}$  [24], confirming the predicted onset of quadrupole deformation below  $^{48}\text{Ca}$ . The shell model has also been applied in the calculation of charge isotope shifts of even and odd Ca isotopes [25]. The model reproduces the characteristic features of the isotope shifts, the parabolic dependence on the mass number and the pronounced odd-even staggering, related to the partial breakdown of the  $Z = 20$  shell closure.

The magicity of the  $N = 40$  shell and, in particular, the possible doubly magic character of  $^{68}\text{Ni}$  has recently attracted considerable interest. The behavior of the  $B(E2, 0^+ \rightarrow 2^+)$  values in the Ni isotopic chain illustrates the structural evolution from the doubly magic nucleus  $^{56}\text{Ni}$  to  $^{68}\text{Ni}$  [26]. Although the latter nucleus does not display a pronounced discontinuity in the two-neutron separation energy, the low-lying  $0_2^+$  level and the marked decrease of the  $B(E2, 0^+ \rightarrow 2^+)$  have been interpreted as evidence for magicity at  $N = 40$ . However, recent microscopic calculations of the  $B(E2)$  strength distribution in even-even Ni isotopes, using the shell model Monte Carlo, the quasiparticle random-phase approximation, and a large-scale diagonalization shell model, have shown that in  $^{68}\text{Ni}$  the calculated  $B(E2)$  value to the first  $2^+$  state exhausts only a fraction of the low-lying  $B(E2)$  strength, and that the small experimental  $B(E2)$  value to the first  $2^+$  state is not a strong evidence for the doubly-magic character of  $^{68}\text{Ni}$  [27].

The proton-rich deformed nuclei in the  $A \approx 80$  mass-region are still beyond the capabilities of the shell-model diagonalization approach. Nevertheless, first shell model Monte Carlo calculations for proton-rich Kr, Sr and Zr isotopes in the mass range  $A = 72 - 84$  have been reported [28]. By employing the complete  $0f1p-0g1d2s$  configuration space, the calculations reproduce the large empirical  $B(E2)$  values, and attribute the ground state deformations to the gain in the correlation energy obtained by promoting nucleons across the  $N = 40$  subshell closure. In heavy systems the evolution of proton shell structure beyond  $^{208}\text{Pb}$  is of decisive importance for the shell stabilization of superheavy elements. Shell model calculations for the  $N = 126$  isotones have been performed for the first time in the full proton  $Z = 82 - 126$  model space [29]. In comparison with experimental data, excellent results have been obtained for binding energies, level schemes and electromagnetic properties.

Properties of heavy nuclei with a large number of active valence nucleons are best described in the framework of self-consistent mean-field methods. A broad range of successful applications to nuclear structure and low-energy dynamics characterizes mean-field models based on the Gogny interaction, the Skyrme energy functional, and the relativistic meson-exchange effective Lagrangian [30]. In recent years important advances have been

reported in the self-consistent mean-field treatment of exotic nuclei far from stability.

A quantitative description of phenomena related to shell evolution necessitates the inclusion of many-body effects beyond the mean-field approximation. The starting point is usually a constrained Hartree-Fock plus BCS (HFBCS), or Hartree-Fock-Bogoliubov (HFB) calculation of the potential energy surface with the mass quadrupole components as constrained quantities. In most applications the calculations have been restricted to axially symmetric, parity conserving configurations. The erosion of spherical shell closures in neutron-rich nuclei produces deformed intrinsic states and, in some cases, mean-field potential energy surfaces with almost degenerate prolate and oblate minima. Soft potential energy surfaces and/or small energy differences between coexisting minima point to the importance of including correlation effects. The rotational energy correction, i.e. the energy gained by the restoration of rotational symmetry, is proportional to the quadrupole deformation of the intrinsic state and can reach few MeV for a well deformed configuration. Fluctuations of the quadrupole deformation also contribute to the correlation energy. Both types of correlations can be included simultaneously by mixing angular momentum projected states corresponding to different quadrupole moments. Configuration mixing is usually performed by using the generator coordinate method (GCM) with the quadrupole deformation as generator coordinate.

In a series of recent papers [31–34], the angular momentum projected GCM with the axial quadrupole moment as the generating coordinate, and intrinsic configurations calculated in the HFB model with the finite range Gogny interaction, has been applied in studies of shape-coexistence phenomena that result from the erosion of the  $N = 20$  and  $N = 28$  spherical shells in neutron-rich nuclei. Based on the well known D1S parameterization of the effective Gogny interaction, the calculations are completely parameter-free. Good agreement with experimental data has been obtained for the  $2^+$  excitation energies and B(E2) transition probabilities of the  $N = 28$  neutron-rich isotones, and coexistence of shapes has been predicted in  $^{42}\text{Si}$ ,  $^{44}\text{S}$ , and  $^{46}\text{Ar}$  [31]. The systematic study of the ground and low-lying excited states of the even-even  $^{20-40}\text{Mg}$  [32] is particularly interesting, because this chain of isotopes includes three spherical magic numbers  $N = 8, 20, 28$ . It has been shown that the  $N = 8$  shell closure is preserved, whereas deformed ground states are calculated for  $N = 20$  and  $N = 28$ . In particular, the ground state of  $^{32}\text{Mg}$  becomes deformed only after the inclusion of the rotational energy correction. The  $0^+$  collective wave function displays significant mixing of oblate and prolate configurations. The deformed ground state of  $^{32}\text{Mg}$  occurs as a result of a fine balance between the zero-point correction associated with the restoration of rotational symmetry and the correlations induced by quadrupole fluctuations. In a similar analysis of the chain of even-even isotopes  $^{20-34}\text{Ne}$  [33], it has been found that the ground state of the  $N = 20$  nucleus  $^{30}\text{Ne}$  is deformed, but less than the ground state of its isotone  $^{32}\text{Mg}$ . The model has recently been applied in an analysis of the shape coexistence and quadrupole collectivity in the neutron-deficient Pb isotopes [34]. A good qualitative agreement with available data has been found, especially for the rotational bands built on coexisting low-lying oblate and prolate states.

Another very sophisticated model [35] which extends the self-consistent mean-field approach by including correlations, is based on constrained HF+BCS calculations with Skyrme effective interactions in the particle-hole channel and a density-dependent contact force in the pairing channel. Particle number and rotational symmetry are restored

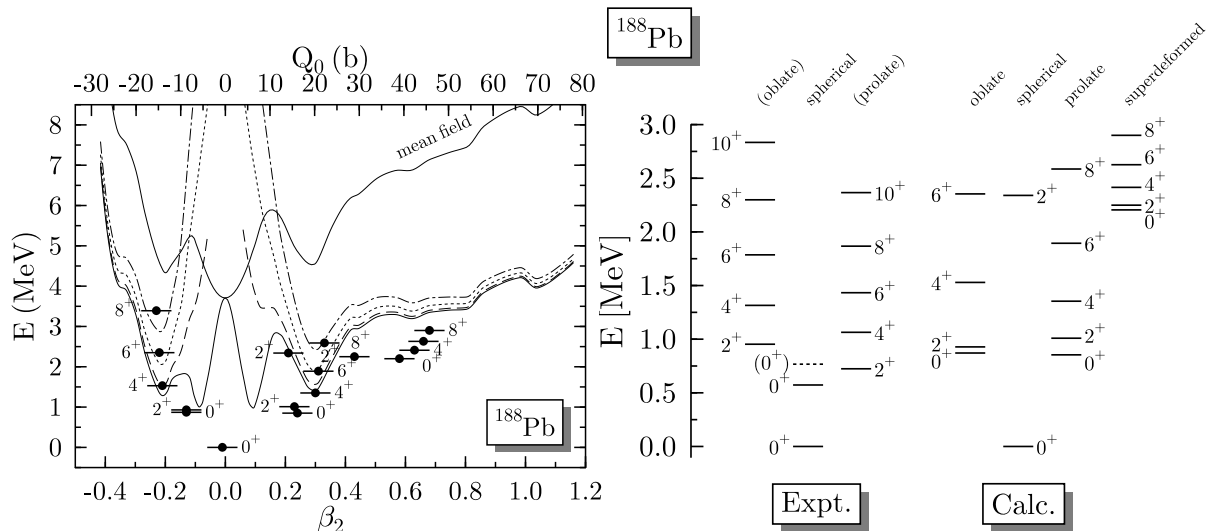


Figure 1. Particle-number projected (mean-field), particle-number and angular-momentum projected potential energy curves up to  $J = 8^+$ , and the corresponding lowest GCM states for  $^{188}\text{Pb}$  as functions of the quadrupole deformation (left panel) [39]. In the right panel the calculated excitation energies are compared with the available experimental data [40].

by projecting the self-consistent mean-field wave functions on the correct numbers of neutrons and protons, and on the angular momentum. Finally, a mixing of the projected wave functions corresponding to different quadrupole moments is performed with a discretized version of the generator coordinate method. The model has recently been successfully tested in the study of shape coexistence in  $^{16}\text{O}$  [36], and in the analysis of the coexistence of spherical, deformed, and superdeformed states in  $^{32}\text{S}$ ,  $^{36}\text{Ar}$ ,  $^{38}\text{Ar}$  and  $^{40}\text{Ca}$  [37]. For the doubly-magic nucleus  $^{16}\text{O}$  this parameter-free approach provides a very good description of those low-spin states that correspond to axially and reflection-symmetric shapes, and allows the interpretation of their structure in terms of self-consistent  $np - nh$  states. A very important recent application is the study of low-lying collective excitation spectra of the neutron-deficient lead isotopes  $^{182-194}\text{Pb}$  [38,39]. A configuration mixing of angular-momentum and particle-number projected self-consistent mean-field states, calculated with the Skyrme SLy6 effective interaction, qualitatively reproduces the coexistence of spherical, oblate, prolate and superdeformed prolate structures in neutron-deficient Pb nuclei. The results are illustrated in Fig. 1, where the GCM spectra of  $^{188}\text{Pb}$  are compared with the recent experimental data [40]. In a shell-model language the excited  $0^+$  states are generated by proton excitations across the  $Z = 82$  spherical shell gap. The mean-field oblate minimum is associated with  $2p - 2h$  proton configurations, and the prolate one with  $4p - 4h$  proton intruder states.

In order to describe pairing correlations in weakly bound nuclei close to the neutron drip line, new methods have been developed that improve the treatment of the continuum coupling in HFB based models [41–43].

The self-consistent mean-field framework, extended to take into account the most im-

portant correlations, provides a detailed microscopic description of structure phenomena associated with the shell evolution in exotic nuclei. When compared to the shell model, important advantages of this approach include the use of global effective nuclear interactions, the treatment of arbitrarily heavy systems including superheavy elements, and the intuitive picture of intrinsic shapes. Further developments will involve additional degrees of freedom as generator coordinates, the description of odd nuclei, the extension to triaxial shapes, the inclusion of negative parity structures, and the use of effective interactions that have been readjusted to take into account the explicit treatment of correlations.

#### 4. Towards a universal energy density functional

The self-consistent mean-field approach to nuclear structure represents an approximate implementation of Kohn-Sham density functional theory (DFT). The DFT enables a description of the nuclear many-body problem in terms of a universal energy density functional, and mean-field models approximate the exact energy functional, which includes all higher-order correlations, with powers and gradients of ground-state nucleon densities. Although it models the effective interaction between nucleons, a general density functional is not necessarily related to any given NN potential. By employing global effective interactions, adjusted to reproduce empirical properties of symmetric and asymmetric nuclear matter, and bulk properties of simple, spherical and stable nuclei, the current generation of self-consistent mean-field methods has achieved a high level of accuracy in the description of ground states and properties of excited states in arbitrarily heavy nuclei, exotic nuclei far from  $\beta$ -stability, and in nuclear systems at the nucleon drip-lines.

Concerning the predictive power of these methods, however, the situation is far from being satisfactory and there are many issues to be addressed. For instance, until very recently global effective interactions were adjusted to ground-state properties of no more than ten or so spherical nuclei. Nuclear masses calculated with these interactions have a typical rms deviation of  $\approx 2$  MeV when compared with experimental mass tables. Even though calculated one- and two-nucleon separation energies for nuclei not far from stability are usually fairly accurate, various non-relativistic and relativistic mean-field models differ significantly in the prediction of separation energies close to the drip lines and, in general, of isovector properties far from stability. It must be also emphasized that global effective interactions have not been optimized to go beyond the mean-field plus pairing approximation and therefore, when used in calculations that explicitly include correlations, they might lead to results that are not completely reliable.

One of the major goals of modern nuclear structure is, therefore, to build a universal energy density functional theory [44]. Universal in the sense that the same functional is used for all nuclei, with the same set of parameters. This framework should then provide a reliable microscopic description of infinite nuclear and neutron matter, ground-state properties of all bound nuclei, low-energy vibrations, rotational spectra, small-amplitude vibrations, and large-amplitude adiabatic properties. The next generation of energy density functionals should move away from model dependence by including all terms allowed by symmetries, and all available data, rather than a small subset of spherical nuclei, should be used in adjusting phenomenological parameters. Properties of nuclei far from stability, in particular, should provide stringent constraints on the isovector channels of



effective nuclear interactions. New interactions in turn will enable an improved description of structure phenomena in exotic systems and more reliable extrapolations toward the drip lines.

The first step in this direction is the construction of microscopic mass tables. Recent trends in the determination of nuclear masses have been reviewed in Ref. [45]. From the theoretical point of view an important advance is the development of self-consistent Skyrme Hartree-Fock (HF) and Skyrme Hartree-Fock-Bogoliubov (HFB) mass formulas. In a series of recent papers [46–49] a set of complete microscopic mass tables of more than 9000 nuclei lying between the particle drip lines over the range  $Z, N \geq 8$  and  $Z \leq 120$ , have been constructed within the HFB framework. By adjusting the parameters of the Skyrme interaction, the strength and the cut-off parameters of the (possibly density-dependent)  $\delta$ -function pairing force, and the parameters of two phenomenological Wigner terms, with a total of  $\approx 20$  parameters in all, the measured masses of 2135 nuclei with  $Z, N \geq 8$  have been fitted with an rms error of less than 700 keV. In addition, although these effective interactions have been adjusted only to masses, they also produce excellent results for the charge radii, with an rms deviation of  $\approx 0.025$  fm for the absolute charge radii and charge isotope shifts of more than 500 nuclei [50]. However, despite the impressive quality of the Skyrme-HFB mass formulas, they are far from being definite, and a number of very recent studies have considered possible modifications to the interactions, a better treatment of symmetry-breaking effects and many-body correlations, and improved methods of calculations. In Ref. [51] an improved version of the deformed configuration-space HFB method has been reported, based on the expansion of the HFB wave functions in a complete set of transformed harmonic-oscillator basis states, obtained by a local-scaling point transformation. This method enables a careful treatment of the asymptotic part of the nucleonic density, and is therefore particularly suitable for self-consistent HFB calculations of deformed weakly-bound nuclei close to the nucleon drip lines. In the first application, the Skyrme force SLy4 and volume pairing have been employed in the calculation of the entire deformed even-even mass table for  $Z \leq 108$  and  $N \leq 188$ , with exact particle number projection following the application of the Lipkin-Nogami prescription.

When considering proton-rich nuclei with  $Z \approx N$ , additional proton-neutron ( $pn$ ) correlations, e.g.  $pn$  pairing, have to be taken into account. Even though the effect of these correlations on the binding energies can be approximated by phenomenological Wigner terms [45–49], it is important to extend the self-consistent mean-field methods to incorporate proton-neutron mixing. In Ref. [52] the coordinate-space HFB framework has been generalized to include arbitrary mixing between protons and neutrons both in the particle-hole and particle-particle channels. The resulting HFB density matrices have a rich spin-isospin structure and provide a microscopic description of pairing correlations in all isospin channels.

In global microscopic mass tables one usually treats various mean-field and pairing effects very carefully, whereas additional correlations, related to the restoration of broken symmetries and to fluctuations, are either neglected or taken into account in a very schematic way. Correlations are, however, very important if the goal is a level of accuracy better than 500 keV. Unfortunately, the standard microscopic methods for treating correlations are computationally far too expensive when applied in calculations involving thousands of nuclei. It will be very useful to develop approximate methods of calculating

correlations, that would reduce the computational cost and therefore enable a systematic calculation of correlation energies for the nuclear mass table [53].

An important class of self-consistent mean-field models belongs to the framework of relativistic mean-field theory (RMF). RMF-based models have been very successfully employed in analyses of a variety of nuclear structure phenomena, not only in nuclei along the valley of  $\beta$ -stability, but also in exotic nuclei with extreme isospin values and close to the particle drip lines. Applications have reached a level of sophistication and accuracy comparable to the non-relativistic Hartree-Fock (Bogoliubov) approach based on Skyrme or Gogny effective interactions. Nevertheless, standard RMF Lagrangians with nonlinear meson self-interactions are plagued with a number of problems, especially when describing isovector properties. Recently it has been shown that much better results are obtained in an effective hadron field theory with medium dependent meson-nucleon vertices. Such an approach retains the basic structure of the relativistic mean-field framework, but can be more directly related to the underlying microscopic description of nuclear interactions. One way to determine the functional form of the meson-nucleon vertices is from in-medium Dirac-Brueckner interactions, obtained from realistic free-space NN interactions. This microscopic approach represents an *ab initio* description of nuclear matter and finite nuclei. The corresponding density-dependent relativistic hadron field model has recently been applied to asymmetric nuclear matter and exotic nuclei [54], hypernuclei [55,56], and neutron star matter [57]. On the other hand, a phenomenological approach was adopted in Ref. [58], where the density dependence for the  $\sigma$ ,  $\omega$  and  $\rho$  meson-nucleon couplings was adjusted to properties of nuclear matter and a set of spherical nuclei. This phenomenological effective interaction was further improved in Ref. [59], where the relativistic Hartree-Bogoliubov (RHB) model was extended to include medium-dependent vertex functions. It has been shown that, in comparison with standard non-linear meson self-interactions, relativistic models with an explicit density dependence of the meson-nucleon couplings provide an improved description of asymmetric nuclear matter, neutron matter and nuclei far from stability. The relativistic random-phase approximation (RRPA), based on effective Lagrangians characterized by density-dependent meson-nucleon vertex functions, has been derived in Ref. [60]. A comparison of the RRPA results on multipole giant resonances with experimental data provide additional constraints on the parameters that characterize the isoscalar and isovector channels of the density-dependent effective interactions. In a microscopic analysis of the nuclear matter compressibility and symmetry energy [61], it has been shown that the experimental data on the giant monopole resonances restrict the nuclear matter compression modulus of structure models based on the relativistic mean-field approximation to  $K_{\text{nm}} \approx 250 - 270$  MeV, while the isovector giant dipole resonances and the available data on differences between neutron and proton radii limit the range of the nuclear matter symmetry energy at saturation (volume asymmetry) of these effective interactions to  $32 \text{ MeV} \leq a_4 \leq 36 \text{ MeV}$ . The RMF framework with minimal meson-nucleon couplings has recently been generalized by introducing couplings of the meson fields to derivatives of the nucleon field in the Lagrangian density [62]. This approach leads to nucleon self-energies that depend on both density and momentum, and enables an effective description of a state-dependent in-medium interaction in the mean-field approximation.

## 5. Exotic modes of excitations

The multipole response of unstable nuclei far from the line of  $\beta$ -stability presents a very active field of research. On the neutron rich side the modification of the effective nuclear potential leads to the formation of nuclei with very diffuse neutron densities, and to the occurrence of the neutron skin and halo structures. These phenomena will also affect the multipole response of unstable nuclei, in particular the electric dipole and quadrupole excitations, and new modes of excitations could arise in nuclei near the drip line. New models have recently been developed that describe the low-lying collective excitations in weakly bound nuclei by explicitly taking into account the coupling to the continuum [63–65].

The dipole response of very neutron-rich isotopes is characterized by the fragmentation of the strength distribution and its spreading into the low-energy region, and by the mixing of isoscalar and isovector modes. It appears that in most relatively light nuclei the onset of dipole strength in the low-energy region is due to non-resonant independent single-particle excitations of the loosely bound neutrons. The structure of the low-lying dipole strength, however, changes with mass and in heavier nuclei low-lying dipole states appear that are characterized by a more distributed structure of the (Q)RPA amplitude. Among peaks characterized by single particle transitions, collective dipole states are identified below 10 MeV, and their amplitudes represent coherent superpositions of many neutron particle-hole configurations. The corresponding transition densities reveal the dynamics of a pygmy dipole resonance (PDR): the neutron skin oscillates against an  $N \approx Z$  core.

The dipole response in neutron-rich oxygen isotopes has attracted considerable interest [66,67]. Low-lying E1 strength has been observed exhausting about 10% of the classical dipole sum rule below 15 MeV excitation energy. Extensive theoretical studies, including large-scale shell-model calculations [68], relativistic (Q)RPA [69,70], and the QRPA plus phonon coupling model [71], reproduce the experimentally observed redistribution of the E1 strength in neutron-rich oxygen isotopes, but they also show that the low-lying dipole states represent a new type of non-resonant independent single-particle excitations, not caused by a coherent superposition of particle-hole ( $ph$ ) configurations like in collective states. The structure of the QRPA amplitudes of all low-lying dipole states is dominated by one, or at most two, single-neutron  $ph$  excitations.

Very recently experimental data have been reported on the concentration of electric dipole strength below the neutron separation energy in  $N = 82$  semi-magic nuclei. The distribution of the electric dipole strength in  $^{138}\text{Ba}$ ,  $^{140}\text{Ce}$ , and  $^{144}\text{Sm}$  displays a resonant structure between 5.5 MeV and 8 MeV, exhausting  $\approx 1\%$  of the isovector E1 energy weighted sum rule [72]. In  $^{138}\text{Ba}$  negative parity quantum numbers have been assigned to 18 dipole excitations between 5.5 MeV and 6.5 MeV [73]. The experimental information available presently, however, does not allow one to determine the dominant structure of the observed states. The Sn isotopes present another very interesting example of the evolution of the low-lying dipole strength with neutron number. The relativistic QRPA has been employed in the analysis of the distribution of dipole strength in Sn isotopes and  $N=82$  isotones [70]. It has been shown that in neutron-rich nuclei a relatively strong peak appears in the dipole response below 10 MeV, with a QRPA amplitude characterized by a coherent superposition of many neutron quasiparticle configurations. This collective

mode represents the oscillation of the skin of excess neutrons against the core composed of an equal number of protons and neutrons: the pygmy dipole resonance. Beyond the QRPA level, the PDR in neutron-rich Sn nuclei has been investigated by employing the Quasiparticle Phonon Model (QPM), which provides a consistent unified description of low-energy single- and multi-phonon states. QPM calculations, including up to three-phonon configurations, have shown that anharmonic admixtures induce a considerable fragmentation of the low-lying E1 strength [74]. Nevertheless, despite significant multi-phonon contributions, the PDR states retain their basically one-phonon character. An important result of the QPM analysis is that the fragmentation pattern is reduced when increasing the neutron excess toward  $^{132}\text{Sn}$ .

Besides being intrinsically interesting as an exotic mode of excitation, the occurrence of the PDR has important implications for the r-process nucleosynthesis. Namely, although the E1 strength of the PDR is small compared to the total dipole strength, if located well below the neutron separation energy the PDR can significantly increase the radiative neutron capture cross section on neutron-rich nuclei, as shown in recent large-scale QRPA calculations of the E1 strength for the whole nuclear chart [75,76].

Pygmy dipole resonances are not necessarily limited to exotic nuclei far from stability. This phenomenon can be expected to occur in all medium-heavy and heavy systems characterized by a significant excess of neutrons. For example, a recent relativistic RPA calculation [77] had predicted the PDR in  $^{208}\text{Pb}$  at the neutron emission threshold. The resonance has been subsequently observed in a high-resolution  $(\gamma, \gamma')$  study of the electric dipole response [78], and the data have been very accurately described in a QPM study with realistic model spaces, including the coupling of up to three-phonon configurations. The QPM analysis of the velocity distributions of the E1 excitations in  $^{208}\text{Pb}$  has shown that the  $1^-$  states close to the particle threshold contain pronounced components that correspond to vortex collective motion. This result is in agreement with the prediction of the occurrence of the toroidal dipole resonance in this energy region [79]. The toroidal dipole mode corresponds to a transverse zero-sound wave and its experimental observation invalidates the hydrodynamical picture of the nuclear medium, since there is no restoring force for such modes in an ideal fluid. Another exotic E1 mode in the energy region below giant resonances has recently been the subject of intensive experimental and theoretical investigation. This is the low-energy component of the isoscalar dipole resonance (ISGDR) (for a recent review of the current experimental work on the ISGDR, see Ref. [80]). Although in a classical picture the ISGDR corresponds to a second order compression mode and therefore provides information on the nuclear matter compression modulus, several theoretical studies [81–84] have predicted the existence of a low-energy component that is not sensitive to the nuclear compressibility.

Of course, not only dipole states characterize the exotic low-energy multipole response of neutron-rich nuclei. Many other interesting phenomena have been observed and analyzed. For example, in certain neutron-rich Te isotopes a decrease in the energy of the first excited  $2^+$  state is accompanied by a decrease in the corresponding  $B(E2, 0^+ \rightarrow 2^+)$ . This behavior of the E2 strength contradicts the simple systematics observed in most isotopic chains, i.e. an increase of the E2 strength as the first excited  $2^+$  state decreases in energy and becomes more collective. In the QRPA analysis of Ref. [85] this anomalous behavior of  $2^+$  excitations around  $^{132}\text{Sn}$  has been attributed to a reduction in the neutron

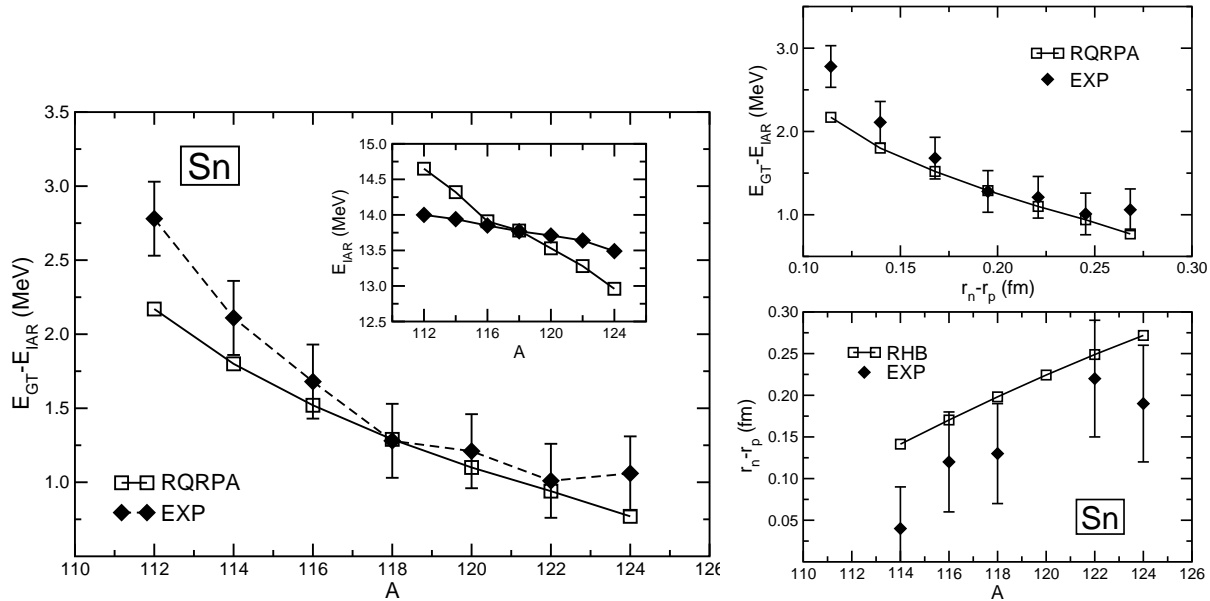


Figure 2. The proton-neutron RQRPA and experimental differences between the excitation energies of the GTR and IAS for the sequence of even-even  $^{112-124}\text{Sn}$  target nuclei, as a function of the mass number (left panel) and of the calculated differences between the rms radii of the neutron and proton density distributions of even-even Sn isotopes (upper right panel). In the lower panel on the right the calculated differences  $r_n - r_p$  are compared with experimental data [87].

pairing above the  $N = 82$  spherical shell gap.

The systematics of low-energy pygmy modes could in principle be used to determine the thickness of the neutron skin in neutron-rich nuclei [70,74]. Two experimental methods based on giant resonances have been used to study the neutron skin: the excitation of the giant dipole resonances (GDR) [86] and the spin-dipole resonance [87]. Recently a new method has been suggested for determining the difference between the radii of the neutron and proton density distributions along an isotopic chain, based on measurement of the excitation energies of the Gamow-Teller resonance (GTR) relative to the isobaric analog state (IAS) [88,89]. The concept is illustrated in Fig. 2, where the results of a relativistic proton-neutron quasiparticle random-phase approximation calculation for the excitation energies of the main component of the GT resonances and the respective isobaric analog states for the sequence of even-even  $^{112-124}\text{Sn}$ , are shown in comparison with data, and the calculated differences  $r_n - r_p$  are compared with experimental values deduced from the excitation of the SDR [87]. For a given effective nuclear interaction which reproduces the ground-state and the excitations of the IAS and the GTR, the correlation shown in Fig. 2 can be used to determine the value of the neutron skin.

The ability to model the Gamow-Teller response is, of course, essential for reliable predictions of  $\beta$ -decay rates in neutron-rich nuclei along the  $r$ -process path. The calculation of GT strength, however, can also be used to constrain the spin-isospin channel of energy density functionals. For the Skyrme energy functionals, an initial analysis of the couplings

of the spin-isospin terms bilinear in time-odd densities and currents, has been reported in Ref. [90]. In the relativistic framework the time-odd channels are not independent from the time-even ones because they arise from the small components of the Dirac spinor and, therefore, a very natural microscopic model for the description of spin-isospin excitations is the proton-neutron relativistic QRPA (PN-RQRPA). In a recent work [89], the PN-RQRPA has been formulated in the canonical single-nucleon basis of the relativistic Hartree-Bogoliubov model, and employed in the analysis of charge-exchange modes in open-shell neutron-rich nuclei, with particular emphasis on the role of the  $T = 1$  and  $T = 0$  pairing channels.

## 6. Microscopic predictions for astrophysical applications

The latest theoretical and computational advances in nuclear structure modeling have also had a strong impact on nuclear astrophysics. More and more often calculations of stellar nucleosynthesis, nuclear aspects of supernova collapse and explosion, and neutrino-induced reactions, are based on microscopic global predictions for the nuclear ingredients, rather than on coarse and oversimplified phenomenological approaches. The nuclear input for astrophysics calculations necessitates the knowledge of the properties of thousands of nuclei far from stability, including the characteristics of strong, electromagnetic and weak interaction processes. Most of these nuclei, especially on the neutron-rich side, are not accessible in experiments and, therefore, many nuclear astrophysics calculations crucially depend on accurate theoretical predictions for the nuclear masses, bulk properties, nuclear excitations,  $(n, \gamma)$  and  $(\gamma, n)$  rates,  $\alpha$ - and  $\beta$ -decay half-lives, fission probabilities, electron and neutrino capture rates, etc.

The path of the  $r$ -process nucleosynthesis runs through regions of very neutron-rich nuclei.  $\beta$ -decays are particularly important because they generate elements with higher  $Z$ -values, and set the time scale of the  $r$ -process. Except for a few key nuclei, however,  $\beta$ -decays of  $r$ -process nuclei have to be determined from nuclear models. Both the shell model and the QRPA have been employed in large-scale calculations of weak rates for the  $r$ -process. Shell model applications in nuclear astrophysics have recently been reviewed in Refs. [91,92]. In the calculation of  $\beta$ -half-lives, in particular, the principal advantage of the shell model is the ability to take into account the detailed structure of the  $\beta$ -strength functions. In addition to large-scale shell model predictions for the half-lives of waiting-point nuclei at  $N = 50, 80, 126$  [92], the no-core shell model [7] and the shell model embedded in the continuum [93] have been applied to  $\beta$ -decay of light nuclei. The self-consistent HFB plus continuum QRPA framework has been employed in a systematic calculation of the allowed and first-forbidden  $\beta$ -decay rates for the  $r$ -process nuclei near  $N = 50, 80, 126$  [94]. It has been shown that the effect of the high-energy first-forbidden transitions is crucial for  $Z \geq 50$ ,  $N \approx 82$ , and especially in the  $N = 126$  region.

Improved large-scale shell model results for weak-interaction rates, both for beta decay and electron capture, have been used in a study of presupernova evolution of massive stars [95]. Compared to standard presupernova models, larger values of the electron-to-baryon ratio at the onset of collapse and smaller iron masses have been predicted, and these can have significant consequences for nucleosynthesis and the supernova explosion mechanism. A new model for calculating electron capture rates on neutron-rich nuclei

has been developed [96], based on a combination of shell model Monte Carlo calculation of temperature-dependent occupation numbers of single-particle orbitals, and RPA calculation of electron capture rates including both allowed and forbidden transitions. The model has been used to calculate rates of electron capture on nuclei with mass numbers  $A = 65 - 112$  for the temperatures and densities characteristic for core collapse [97]. It has been shown that, in contrast to previous assumptions, these rates are so large that electron capture on neutron-rich nuclei dominates over capture on free protons. With realistic treatment of electron capture on heavy nuclei, significant changes in the hydrodynamics of core collapse and the properties of the core at bounce have been predicted [98].

Neutrino-induced reactions on heavy neutron-rich nuclei in the post collapse supernova environment could play an important role in the  $r$ -process. In a very recent calculation of neutrino-induced fission cross sections in competition with neutron emission [99], it has been shown that neutrino charged-current capture-induced fission could have a pronounced effect on the nuclear reaction flow paths and nuclear abundances in the  $r$ -process.

## 7. Nuclear structure as an Effective Field Theory of low-energy QCD

The most fundamental problem in theoretical nuclear physics is: how to establish a relationship between low-energy, non-perturbative QCD and the rich nuclear phenomenology which includes both nuclear matter and finite nuclei? The success of the non-relativistic and covariant self-consistent mean-field approach to nuclear many-body dynamics, and the recent application of chiral effective field theory to nucleon-nucleon scattering and the few-body problem, point to a unified microscopic framework based on density functional theory (DFT) and effective field theories (EFT).

At the energy and momentum scales characteristic of nuclei, QCD is realized as a theory of pions coupled to nucleons. The basic concept of a low-energy EFT is the separation of scales: the long-range physics is treated explicitly (e.g. pion exchange) and short-distance interactions, that cannot be resolved at low-energy, are replaced by contact terms. In principle, all interaction terms allowed by symmetries must be included and the EFT framework, i.e. power counting for diagrams and gradient expansions, can be used to remove model dependence. EFT building of the universal microscopic energy density functional allows error estimates to be made, and it also provides a power counting scheme which separates long- and short-distance dynamics. Recent investigations [100–103] have shown that models based on EFT and DFT provide a systematic framework for nuclear structure theory. A novel microscopic covariant description of nuclear many-body dynamics constrained by chiral symmetry and in-medium QCD sum rules has been developed [104,105]. It has been shown that nuclear binding and saturation are essentially generated by chiral (two-pion exchange) fluctuations in combination with Pauli effects, whereas strong scalar and vector fields of about equal magnitude and opposite sign, induced by changes of the QCD vacuum in the presence of baryonic matter, generate the large effective spin-orbit potential in finite nuclei. Promising results have been obtained for the nuclear matter equation of state and for the bulk and single-nucleon properties of finite nuclei. A quantitative *ab initio* description of the nuclear many-body problem, starting from the fundamental theory of QCD, should become feasible in the near future.

## REFERENCES

1. Steven C. Pieper and R. B. Wiringa, *Annu. Rev. Nucl. Part. Sci.* 51 (2001) 51.
2. R. B. Wiringa, V. G. J. Stoks, and R. Schiavilla, *Phys. Rev. C* 51 (1995) 38.
3. Steven C. Pieper, V. R. Pandharipande, R. B. Wiringa, and J. Carlson, *Phys. Rev. C* 64 (2001) 014001.
4. Steven C. Pieper, K. Varga, and R. B. Wiringa, *Phys. Rev. C* 66 (2002) 044310.
5. J. Carlson, J. Morales, Jr., V. R. Pandharipande, and D. G. Ravenhall, *Phys. Rev. C* 68 (2003) 025802.
6. S. Fantoni, A. Sarsa, and K. E. Schmidt, *Phys. Rev. Lett.* 87 (2001) 181101.
7. E. Caurier, P. Navrátil, W. E. Ormand, and J. P. Vary, *Phys. Rev. C* 66 (2002) 024314.
8. P. Navrátil and W. E. Ormand, *Phys. Rev. Lett.* 88 (2002) 152502.
9. P. Navrátil and W. E. Ormand, *Phys. Rev. C* 68 (2003) 034305.
10. P. Navrátil and E. Caurier, *Phys. Rev. C* 69 (2004) 014311.
11. D. R. Entem and R. Machleidt, *Phys. Rev. C* 68 (2003) 041001(R).
12. E. Caurier, G. Martínez-Pinedo, F. Nowacki, A. Poves, and A. P. Zuker, arXiv:nucl-th/0402046 (2004).
13. A. P. Zuker, *Phys. Rev. Lett.* 90 (2003) 042502.
14. A. Poves, J. Sánchez-Solano, E. Caurier, and F. Nowacki, *Nucl. Phys. A* 694 (2001) 157.
15. M. Honma, T. Otsuka, B. A. Brown, and T. Mizusaki, *Phys. Rev. C* 65 (2002) 061301(R); *Phys. Rev. C* 69 (2004) 034335.
16. N. Michel, W. Nazarewicz, M. Ploszajczak, and K. Bennaceur, *Phys. Rev. Lett.* 89 (2002) 042502.
17. N. Michel, W. Nazarewicz, M. Ploszajczak, and J. Okolowicz, *Phys. Rev. C* 67 (2003) 054311.
18. N. Michel, W. Nazarewicz, M. Ploszajczak, and J. Rotureau, arXiv:nucl-th/0401036 (2004).
19. J. Dukelsky, S. Pittel, S. S. Dimitrova, and M. V. Stoitsov, *Phys. Rev. C* 65 (2002) 054319.
20. T. Otsuka, R. Fujimoto, Y. Utsuno, B. A. Brown, M. Honma, and T. Mizusaki, *Phys. Rev. Lett.* 87 (2001) 082502.
21. A. P. Zuker, *Phys. Rev. Lett.* 91 (2003) 179201; T. Otsuka *et al.*, *Phys. Rev. Lett.* 91 (2003) 179202.
22. S. N. Liddick *et al.*, *Phys. Rev. Lett.* 92 (2004) 072502.
23. T. Suzuki, R. Fujimoto, and T. Otsuka, *Phys. Rev. C* 67 (2003) 044302.
24. D. Sohler *et al.*, *Phys. Rev. C* 66 (2002) 054302.
25. E. Caurier, K. Langanke, G. Martínez-Pinedo, F. Nowacki, and P. Vogel, *Phys. Lett. B* 522 (2001) 240.
26. O. Sorlin *et al.*, *Phys. Rev. Lett.* 88 (2002) 092501.
27. K. Langanke, J. Terasaki, F. Nowacki, D. J. Dean, and W. Nazarewicz, *Phys. Rev. C* 67 (2003) 044314.
28. K. Langanke, D. J. Dean, and W. Nazarewicz, *Nucl. Phys. A* 728 (2003) 109.
29. E. Caurier, M. Rejmund, and H. Grawe, *Phys. Rev. C* 67 (2003) 054310.
30. M. Bender, P.-H. Heenen, and P.-G. Reinhard, *Rev. Mod. Phys.* 75 (2003) 121.



31. R. Rodríguez-Guzmán, J. L. Egido, and L. M. Robledo, Phys. Rev. C 65 (2002) 024304.
32. R. Rodríguez-Guzmán, J. L. Egido, and L. M. Robledo, Nucl. Phys. A 709 (2002) 201.
33. R. Rodríguez-Guzmán, J. L. Egido, and L. M. Robledo, Eur. Phys. J. A 17 (2003) 37.
34. R. Rodríguez-Guzmán, J. L. Egido, and L. M. Robledo, Phys. Rev. C 69 (2004) 054319.
35. A. Valor, P.-H. Heenen, and P. Bonche, Nucl. Phys. A 671 (2000) 145.
36. M. Bender and P.-H. Heenen, Nucl. Phys. A 713 (2003) 390.
37. M. Bender, H. Flocard, and P.-H. Heenen, Phys. Rev. C 68 (2003) 044321.
38. T. Duguet, M. Bender, P. Bonche, and P.-H. Heenen, Phys. Lett. B 559 (2003) 201.
39. M. Bender, P. Bonche, T. Duguet, and P.-H. Heenen, Phys. Rev. C 69 (2004) 064303.
40. G. D. Dracoulis *et al.*, Phys. Rev. C 67 (2003) 051301(R).
41. M. Grasso, N. Sandulescu, N. Van Giai, and R. J. Liotta, Phys. Rev. C 64 (2001) 064321.
42. M. Grasso, N. Van Giai, and N. Sandulescu, Phys. Lett. B 535 (2002) 103.
43. K. Bennaceur, J. F. Berger, and B. Ducomet, Nucl. Phys. A 708 (2002) 205.
44. G. A. Lalazissis, P. Ring, and D. Vretenar (Eds.), Extended Density Functionals in Nuclear Structure Physics, Lecture Notes in Physics 641, Springer, Heidelberg, 2004.
45. D. Lunney, J. M. Pearson, and C. Thibault, Rev. Mod. Phys. 75 (2003) 1021.
46. M. Samyn, S. Goriely, P.-H. Heenen, J. M. Pearson, and F. Tondeur, Nucl. Phys. A 700 (2002) 142.
47. M. Samyn, S. Goriely, and J. M. Pearson, Nucl. Phys. A 725 (2003) 69.
48. S. Goriely, M. Samyn, P.-H. Heenen, J. M. Pearson, and F. Tondeur, Phys. Rev. C 66 (2002) 024326.
49. S. Goriely, M. Samyn, M. Bender, and J. M. Pearson, Phys. Rev. C 68 (2003) 054325.
50. F. Buchinger, J. M. Pearson, and S. Goriely, Phys. Rev. C 64 (2001) 067303.
51. M. V. Stoitsov, J. Dobaczewski, W. Nazarewicz, S. Pittel, and D. J. Dean, Phys. Rev. C 68 (2003) 054312.
52. E. Perlinska, S. G. Rohoziński, J. Dobaczewski, and W. Nazarewicz, Phys. Rev. C 69 (2004) 014316.
53. M. Bender, G. F. Bertsch, and P.-H. Heenen, Phys. Rev. C 69 (2004) 034340.
54. F. Hofmann, C. M. Keil, and H. Lenske, Phys. Rev. C 64 (2001) 034314.
55. C. M. Keil, F. Hofmann, and H. Lenske, Phys. Rev. C 61 (2000) 064309.
56. C. M. Keil and H. Lenske, Phys. Rev. C 66 (2002) 054307.
57. F. Hofmann, C. M. Keil, and H. Lenske, Phys. Rev. C 64 (2001) 025804.
58. S. Typel and H. H. Wolter, Nucl. Phys. A 656 (1999) 331.
59. T. Nikšić, D. Vretenar, P. Finelli, and P. Ring, Phys. Rev. C 66 (2002) 024306.
60. T. Nikšić, D. Vretenar, and P. Ring, Phys. Rev. C 66 (2002) 064302.
61. D. Vretenar, T. Nikšić, and P. Ring, Phys. Rev. C 68 (2003) 024310.
62. S. Typel, T. v. Chossy, and H. H. Wolter, Phys. Rev. C 67 (2003) 034002.
63. K. Hagino and H. Sagawa, Nucl. Phys. A 695 (2001) 82.
64. M. Matsuo, Nucl. Phys. A 696 (2001) 371.
65. E. Khan, N. Sandulescu, M. Grasso, and N. Van Giai, Phys. Rev. C 66 (2002) 024309.
66. A. Leistenschneider *et al.*, Phys. Rev. Lett. 86 (2001) 5442.

67. E. Tryggestad *et al.*, Phys. Lett. B 541 (2002) 52.
68. H. Sagawa and T. Suzuki, Phys. Rev. C 59 (1999) 3116.
69. D. Vretenar, N. Paar, P. Ring, and G. A. Lalazissis, Nucl. Phys. A 692 (2001) 496.
70. N. Paar, P. Ring, T. Nikšić, and D. Vretenar, Phys. Rev. C 67 (2003) 034312.
71. G. Coló and P. F. Bortignon, Nucl. Phys. A 696 (2001) 427.
72. A. Zilges, S. Volz, M. Babilon, T. Hartmann, P. Mohr, and K. Vogt, Phys. Lett. B 542 (2002) 43.
73. N. Pietralla *et al.*, Phys. Rev. Lett. 88 (2002) 012502.
74. N. Tsoneva, H. Lenske, and Ch. Stoyanov, Phys. Lett. B 586 (2004) 213.
75. S. Goriely and E. Khan, Nucl. Phys. A 706 (2002) 217.
76. S. Goriely, E. Khan, and M. Samyn, Nucl. Phys. A 739 (2004) 331.
77. D. Vretenar, N. Paar, P. Ring, and G. A. Lalazissis, Phys.Rev. C 63 (2001) 047301.
78. N. Ryezayeva *et al.*, Phys. Rev. Lett. 89 (2002) 272502.
79. D. Vretenar, N. Paar, P. Ring, and T. Nikšić, Phys.Rev. C 65 (2002) 021301(R).
80. U. Garg, Nucl. Phys. A 731 (2004) 3.
81. G.Colò, N. Van Giai, P. F. Bortignon and M. R. Quaglia, Phys. Lett. B 485 (2000) 362.
82. D. Vretenar, A. Wandelt, and P. Ring, Phys. Lett. B 487 (2000) 334.
83. J. Piekarewicz, Phys.Rev. C 64 (2001) 024307.
84. S. Shlomo and A. I. Sanzhur, Phys.Rev. C 65 (2002) 044310.
85. J. Terasaki, J. Engel, W. Nazarewicz, and M. Stoitsov, Phys.Rev. C 66 (2002) 054313.
86. A. Krasznahorkay *et al.*, Phys. Rev. Lett. 66 (1991) 1287; Nucl. Phys. A 567 (1994) 521.
87. A. Krasznahorkay *et al.*, Phys. Rev. Lett. 82 (1999) 3216.
88. D. Vretenar, N. Paar, T. Nikšić, and P. Ring, Phys. Rev. Lett. 91 (2003) 262502.
89. N. Paar, T. Nikšić, D. Vretenar, and P. Ring, Phys.Rev. C 69 (2004) 054303.
90. M. Bender, J. Dobaczewski, J. Engel, and W. Nazarewicz, Phys.Rev. C 65 (2002) 054322.
91. K. Langanke and G. Martínez-Pinedo, Nucl. Phys. A 704 (2002) 154.
92. K. Langanke and G. Martínez-Pinedo, Rev. Mod. Phys. 75 (2003) 819.
93. N. Michel, J. Okolowicz, F. Nowacki, and M. Ploszajczak, Nucl. Phys. A 703 (2002) 202.
94. I. N. Borzov, Phys.Rev. C 67 (2003) 025802.
95. A. Heger, K. Langanke, G. Martínez-Pinedo, and S. E. Woosley, Phys. Rev. Lett. 86 (2001) 1678.
96. K. Langanke, E. Kolbe, and D. J. Dean, Phys.Rev. C 63 (2002) 032801(R).
97. K. Langanke *et al.*, Phys. Rev. Lett. 90 (2003) 241102.
98. W. R. Hix *et al.*, Phys. Rev. Lett. 91 (2003) 201102.
99. E. Kolbe, K. Langanke, and G. M. Fuller, Phys. Rev. Lett. 92 (2004) 111101.
- 100.H. W. Hammer and R. J. Furnstahl, Nucl. Phys. A 678 (2000) 277.
- 101.N. Kaiser, S. Fritsch, and W. Weise, Nucl. Phys. A 697 (2002) 255.
- 102.N. Kaiser, S. Fritsch and W. Weise, Nucl. Phys. A 700 (2002) 343.
- 103.S. Puglia, A. Bhattacharyya, and R. J. Furnstahl, Nucl. Phys. A 723 (2003) 145.
- 104.P. Finelli, N. Kaiser, D. Vretenar, and W. Weise, Eur. Phys. J. A 17 (2003) 573.
- 105.P. Finelli, N. Kaiser, D. Vretenar, and W. Weise, Nucl. Phys. A 735 (2004) 449.